Jurnal Teknologi

Full Paper

A COMPARATIVE STUDY ON METAL-ORGANIC FRAMEWORKS (MOFS) AND METAL OXIDE-BASED ADSORBENTS FOR CO_2 CAPTURE

Nor Khonisah Daud*, Jeevan Rajh A/L Seetha Raman, Ilya Syuhada Rosli

Faculty of Chemical and Process Engineering Technology, Universiti Malaysia Pahang Al-Sultan Abdullah, Lebuh Tun Khalil Yaakob, 26300 Kuantan, Pahang, Malaysia

Article history
Received
2 March 2024
Received in revised form
3 February 2025
Accepted
24 February 2025
Published Online
24 October 2025

*Corresponding author
khonisah@umpsa.edu.my

Graphical abstract

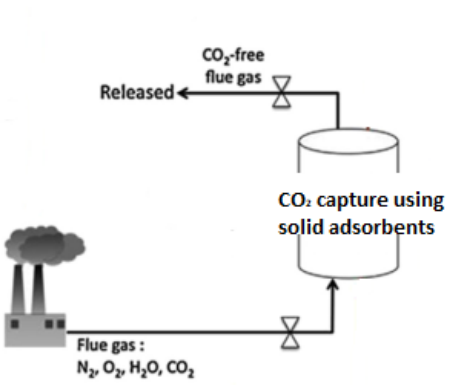

Abstract

Energy sectors, mainly fossil fuel-fired power plants, contribute to the largest proportion of CO_2 production than any other sector. Thus, employing the carbon capture and sequestration (CCS) method in this industry over new or existing facilities has the possibility for the largest reduction in CO_2 emissions compared with other industries. The primary focus of this analysis was to assess the effectiveness of two types of solid adsorbents, metal-organic frameworks (MOFs) (Mg-MOF-74, Zn-MOF), and metal oxide (CuO) for the CO_2 adsorption process. Scanning Electron Microscope (SEM), Fourier Transform Infra-Red (FTIR), Thermal Gravimetric Analyzer (TGA), Energy Dispersive X-ray (EDX), Brunner Emmet Teller (BET), and X-ray Diffraction (XRD) were applied to characterize the developed adsorbents. From the characterization findings, the analyses affirm the development of Mg-MOF-74, Zn-MOF, and CuO. The effectiveness of the prepared adsorbents was investigated as a function of the test variables: impact of pressure and adsorbent amount. The optimum conditions obtained for the CO_2 uptake process for both types of adsorbents were 0.2 g of material amount and 3-4 bar pressure at room condition. Under the optimal parameters, Mg-MOF-74 showed the greatest CO_2 adsorption uptake compared to other adsorbents within 150 min of adsorption time. The experimental results offer a deeper understanding of CO_2 adsorption in the capturing point of a CCS process. The formulation of novel solid adsorbent materials for CO_2 adsorption is also considered the Holy Grail by researchers.

Keywords: Carbon Capture and Sequestration (CCS), CO_2 adsorption uptake, Solid Adsorbents, metal-organic frameworks (MOFs), metal oxide

Abstrak

Sektor tenaga, terutamanya loji janakuasa bahan api fosil menyumbang kepada bahagian terbesar pengeluaran CO_2 berbanding sektor lain. Oleh itu, menggunakan kaedah penangkapan dan penyerapan karbon (CCS) kepada industri ini berbanding kemudahan baharu atau sedia ada mempunyai kemungkinan pengurangan terbesar dalam pelepasan CO_2 berbanding dengan industri lain. Matlamat utama penyelidikan ini adalah untuk membandingkan prestasi pelbagai jenis penjerap pepejal, rangka kerja logam-organik (MOF) (Mg-MOF-74, Zn-MOF) dan oksida logam (CuO) untuk proses penjerapan CO_2. Mengimbas Mikroskop Elektron (SEM), Fourier Transform Infra-Red (FTIR), Penganalisis Gravimetrik Termal (TGA), X-ray Penyerakan Tenaga (EDX), Brunner Emmet Teller (BET) dan Belauan X-ray (XRD) digunakan untuk mencirikan penjerap yang disediakan. Daripada keputusan pencirian, analisis mengesahkan pembangunan Mg-MOF-74, Zn-MOF dan CuO. Keberkesanan bahan penjerap yang disediakan telah disiasat sebagai

fungsi pembolehubah ujian: kesan tekanan dan jumlah penjerap. Keadaan optimum yang diperolehi untuk proses penyerapan CO_2 bagi semua penjerap ialah 0.2 g jumlah penjerap dan tekanan 3-4 bar pada suhu bilik. Di bawah keadaan optimum, Mg-MOF-74 menunjukkan kapasiti penjerapan CO_2 tertinggi berbanding penjerap lain dalam tempoh 150 minit masa penjerapan. Keputusan eksperimen memberikan pemahaman yang lebih baik tentang penjerapan CO_2 dalam menangkap titik proses CCS. Pembangunan bahan penjerap pepejal baru untuk penjerapan CO_2 juga dianggap sebagai 'Holy Grail' oleh para penyelidik.

Kata kunci: Penangkapan dan Penyerapan Karbon (CCS), Penyerapan CO_2, Penjerap Pepejal, rangka kerja logam-organik (MOF), oksida logam

1.0 INTRODUCTION

By the middle of the century (2050), net anthropogenic carbon dioxide (CO_2) emissions must be close to zero to achieve the international efforts' goal of stabilizing the global mean temperature [1]. However, the ongoing development of fossil fuel-burning electricity infrastructure indicates that future CO_2 emissions have already been committed. The increased industrialization associated with cement and lime sectors also adds to the hysterical release of CO_2 into the ambience. Every year, the amount of CO_2 in the environment rises, enhancing the natural greenhouse impact and warming up the world. Therefore, Carbon Capture and Sequestration (CCS) has been introduced to reduce the concentration of CO_2 that has been released. CCS has been adopted as a promising method for reducing, controlling, and storing excessive CO_2 emissions into the atmosphere [2]. Each CCS method is unique in each category of sources of carbon emissions, for example pre-combustion, post-combustion, and oxygenated fuel combustion. For instance, pre-combustion techniques include Integrated Gasification Combined Cycle (IGCC) power plants, hydrate-based technologies, and sorption. In terms of post-combustion, the CO_2 separation techniques presently offered involve absorption, adsorption, cryogenic, and membrane techniques such as MEA distillation and purification. Adsorption seems to be a far better alternative and efficient process for CO_2 capturing due to its favorable characteristics, lower cost, and less capture constraints [3, 4, 5]. The solid adsorbents that are commonly used in adsorption are activated carbon, zeolites, alumina, metal oxides and metal-organic frameworks (MOFs) [6]. Thus, in the present study, the adsorption technique is preferred to be used to capture CO_2 gas.

MOFs are gaining popularity in CO_2 capture due to their great porosity and specific surface area. MOFs also have well-ordered and characterized porous structure together with their adjustable chemical functionality that can be adjusted according to our needs. Besides, the performance of the MOFs can also be altered by improving its CO_2 selectivity through different combinations of metal clusters and organic ligands or both. Alterations in structure and kind of organic ligand (for example phosphonates, imidazolates and carboxylates) as well as metal (i.e., Ca, Fe, Ag, Mg and Zn) lead to development of those MOFs that have the most permeable porosities, providing them ideal alternatives to capture and store gas [7]. Copper oxide (CuO) nanoparticles have gotten a lot of attention because copper is one of the most significant elements in current technology and is easily accessible [8]. Copper oxides are remarkably appealing among all metal oxides for improving the gas adsorption capabilities of AC and/or other solid adsorbents. This is mostly because copper oxides, as compared to other metal oxides, demand lower temperatures for both CO_2 collection and regeneration. CuO is believed to have much superior performance on CO_2 adsorption than copper (I) oxide (Cu_2O) due to its higher electronegativity and specific exterior surface area contrasted to Cu_2O [9]. Table 1 reviews some of the latest works on the CO_2 uptake applying Mg-MOF-74, Zn-MOF and CuO adsorbents.

Yet, there is a lack of comparative works that have been carried out for the efficacy of two different types of materials (metal oxide and MOFs) for CO_2 adsorption and separation purposes. So, there would be worthwhile looking at and comparing efficiencies of CuO, Zn-MOF and Mg-MOF-74 adsorbents in their CO_2 adsorption process. The Mg-MOF-74, Zn-MOF and CuO solid adsorbents were developed and characterized to define the physical and chemical characteristics. The performance of the developed adsorbents was investigated and compared by studying the influence of quantity of adsorbent and pressure on the CO_2 uptake process.

Table 1 List of latest works on the CO_2 uptake with modified adsorbents

Adsorbent	Experimental conditions	Adsorption uptake	Ref.
Mg-MOF-74	CO_2/N_2 (15:85 v/v), room temperature, 0.5 g of Mg-MOF-74 adsorbent were in a U-type stainless steel reactor (1.27 cm ID and 45 cm length). The gases were flowed through the chamber at a flowrate of 10 mLmin^{-1}.	Adsorption of CO_2 from Mg-MOF-74 (S) at 298 K was 350 mgg^{-1}.	[10]
Mg-MOF-74	298 K and 1 bar	8.61 mmolg^{-1}	[11]
Mg-MOF-74, amine grafted MOF-74 (MOF-74-AMP)	298.2 K and 103.58 kPa	Amine embedded MOF-74 (MOF-74-AMP) has greater CO_2 uptake with 0.0046 mol/g as contrasted to MOF-74 with 0.002 mol/g	[12]
Zn-based-MOF material (Zn-URJC-8)	25 and 45 °C	1.28 and 0.74 mmolg^{-1}	[13]
Zn(II) metal–organic framework	273 K under 1 atm	CO_2 adsorption capacity of 92.1 cm^{3}g^{-1}	[14]
MOF-FNP-MeOH and MOF-FNP-H_2O	1 atm and 298 K	The maximum CO_2 adsorption capacity of 3.28 mmolg^{-1} an d 4.09 mmolg^{-1}	[15]
CuO	25 °C	318 mg_{CO_2} g^{-1}	[16]
CuO and Cu_2O	25 °C	9.5 mmol CO_2	[17]

2.0 METHODOLOGY

2.1 Chemicals and Materials

Chemicals and materials used in the preparation of adsorbents were Magnesium Nitrate Hexahydrate $Mg(NO_3)_2 \cdot 6H_2O$, 2,5-Dihydroxyterephthalic Acid, Dimethylformamide (DMF), Ethanol, Methanol, Sodium Hydroxide, Copper (II) Chloride, 1,3,5 – tricarboxylate, $Zn(NO_3)_2 \cdot 6H_2O$ and deionized water. All the chemicals were purchased from Capital Eng. Resource Sdn Bhd.

2.2 Formulation of Adsorbents

2.2.1 Formulation of Mg-MOF-74

In the formulation of Mg-MOF-74, 1.424 g of $Mg(NO_3)_2 \cdot 6H_2O$ as well as 0.334 g of 2,5-Dihydroxyterephthalic acid were balanced and located in a beaker. Then, 135 mL of DMF was added into 9 mL of ethanol and deionised water, respectively with the ratio of 15:1:1. $Mg(NO_3)_2 \cdot 6H_2O$ and 2,5-Dihydroxyterephthalic acid were liquefied in the solution of DMF, ethanol and deionized water and was kept insonication for 30 minutes. The solution was dried in a 125 °C muffle oven for 26 hours prior to cooling to ambient temperature. The concentrated solution was separated and substituted with methanol twice per day for 3 days. The product was heated up in a furnace at 300 ˚C for couple hours before leaving to cool down to ambient conditions. The solid obtained was crushed to finer form and stored.

2.2.2 Formulation of CuO

In the formulation of CuO, 10 g of Copper Chloride ($CuCl_2$) were weighed and mixed with 7 mL of NaOH to yield Copper Hydroxide ($Cu(OH)_2$) solution before put in the oven at 200 °C for 4 hours. The material was further crushed to Copper Oxide adsorbent in a powder form. The copper oxide adsorbent was then stored at room temperature in a sampling bag.

2.2.3 Formulation of Zn-MOF

In the preparation of Zn-MOF, the adsorbent was formulated by liquefying of 1,3,5 – tricarboxylate in 12 mL of ethanol at room temperature. Then, 9 g of $Zn(NO_3)_2 \cdot 6H_2O$ in 12 mL of water was mixed in the prepared solution and stirred continuously before dried at 120 °C overnight. The resulting powder was subsequently heated in an oven at 200 °C for 4 hours.

2.3 Characterization of Adsorbents

The surface morphology of the developed materials was characterized by a Leo Supra VP Field Emission SEM at 20 kV employing a beam size of 3 and high-vacuum conditions, and a ZEISS Merlin High-Resolution SEM at 5-20 kV. Energy dispersive X-ray spectroscopy (EDX) was carried out applying the Oxford INCA 400 for the elemental analysis. FTIR spectroscopy was accomplished to investigate the surface functional groups employing Perkin Elmer FTIR-2000. The blend of KBr to adsorbent was fixed at 1:10 mg. The specimens were tested, and spectra in the span of 4000 to 500 cm^{-1} were documented. The thermogravimetric analyser (TGA) model SDTGA1200

was used to define the thermal stability of adsorbents from 25 °C to 900 °C under N_2 conditions at a constant rate of 5 °C/min. X-ray diffractometer was applied to assess crystalline phase (XRDynamic 500 diffractometer). The scanning was carried out at a diffraction angle of 2-theta with an extend of 5 ° to 60 °. The BET surface area was reached using Micromeritics ASAP 2020 with N_2 adsorption at 77K.

2.4 CO_2 Uptake Process

The CO_2 adsorption uptake was executed employing a fabricated stainless-steel column as a reactor. The reactor was linked to an instrument panel for demonstrating the operating temperature and pressure during the reaction. The tests were initially performed without the application of adsorbents to acquire pure CO_2 concentration. Subsequently, a significant dose of adsorbent was loaded in the reactor prior to the initial temperature and pressure adjustment. The adsorption process occurred after CO_2 was flowed and achieved the required pressure and temperature. The output gas was stored using a Tedlar bag and the concentration was determined by Agilent 6890 FID gas chromatography. After pre-determined time span, the quantity of CO_2 uptake during any time interval was calculated in such a way:

$$q_e = (V(C_o - C_t))/m \quad (1)$$

where q_e is the amount of CO_2 uptake ($mg_{CO2}/g_{adsorbent}$), C_o and C_t are respectively the CO_2 concentration of initial and subsequent times in mg/L. Parameters V and m indicate the size of the chamber (L) and the quantity of material (g) used. The impact of pressure (1-4 bar) and the amount of adsorbent (0.2-0.6 g) on CO_2 adsorption was performed and reviewed periodically.

3.0 RESULTS AND DISCUSSION

3.1 Characterization of Solid Adsorbents

3.1.1 Scanning Electron Microscope (SEM)

The morphology and structure of surfaces of Mg-MOF-74, CuO and Zn-MOF were monitored by SEM and depicted in Figure 1 with different magnifications. As can be seen in Figures 1(a) and (b), the SEM micrographs of Mg-MOF-74 show that the adsorbent had a rough and uneven exterior with porous structure. The particles can be further described having aggregate of cauliflower shaped morphology which represents the Mg-MOF-74 particles.

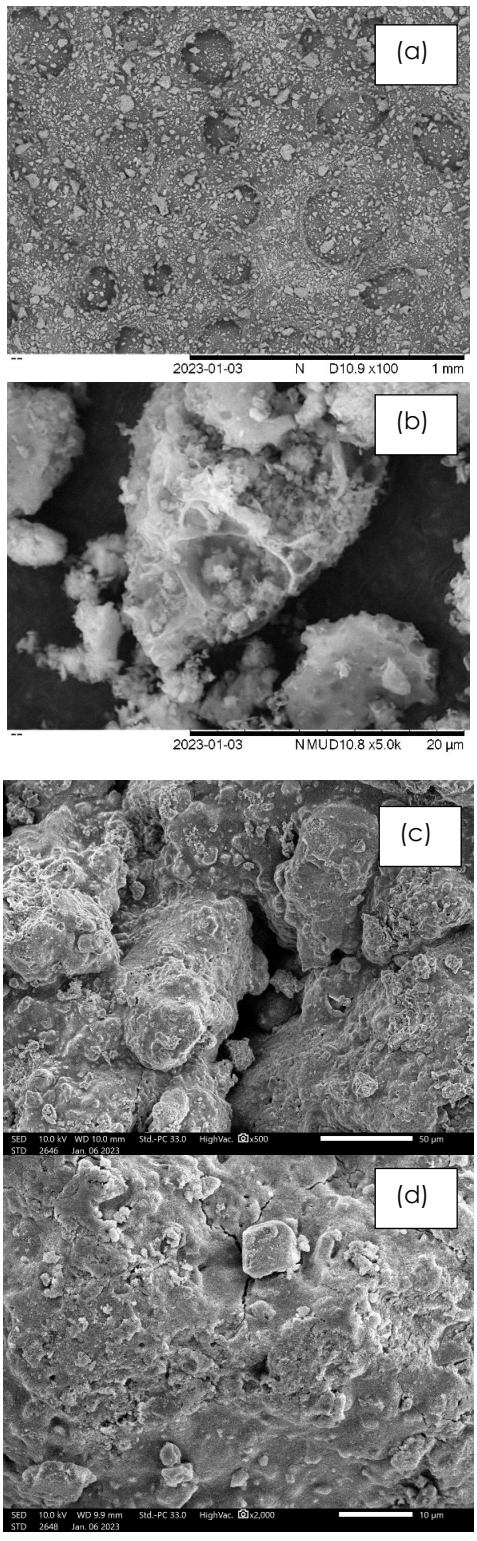

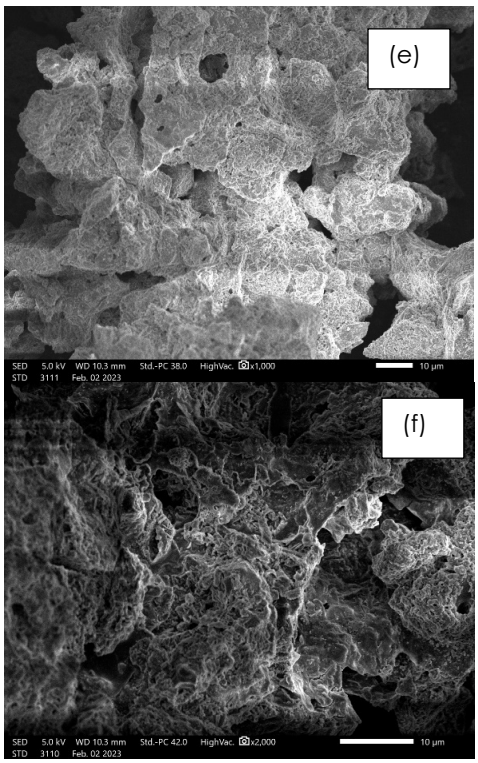

Figure 1 SEM micrographs of (a) 100x Mg-MOF-74, (b) 5000x Mg-MOF-74, (c) 500x CuO, (d) 2000x CuO, (e) 1000x Zn-MOF and (f) 2000x Zn-MOF

The SEM images (Figures 1(c) and (d)) are the images of CuO adsorbent having resolution at 500x and 2000x, respectively. From the images, it is clearly seen that the surface is not smoother. The particles are getting agglomerated due to atomic diffusion because of the heat treatment during preparation of the sample.

Figures 1(e) and (f) display the SEM images of Zn-MOF which exhibit a rough and uneven surface. Also, the crystals agglomerated together on the surface increase the overall particle size of Zn-MOF.

3.1.2 Energy-dispersive X-ray Spectroscopy Analysis (EDX)

The elementary components and purity of the synthesized adsorbents were explored with EDX, as shown in Table 2. The EDX spectra of Mg-MOF-74 shows that on the surface of adsorbent, elements such as Oxygen, Magnesium and Carbon were mostly present. Oxygen has the greatest ratio followed by Magnesium and Carbon. The existence of these components proves the successful synthesis of Mg-MOF-74 as these components will build charges on the exterior surface of the synthesized adsorbent which contributes to CO_2 uptake process [18]. The results were similar to those reported by Xin *et al.* [19], with both studies showing that Mg-MOF-74 had a high ratio of Oxygen, followed by Magnesium and Carbon. The EDX spectra also depicts the existence of other components like Potassium and Calcium at very minimal concentration representing impurities.

In addition, CuO adsorbents contain Copper and Oxygen as the major compounds. When the adsorbent was produced, chlorine compounds are formed from copper (II) chloride when synthesizing the adsorbent. There are additional contaminants such as ferrum and calcium which come during the synthetization process of CuO. The composition of Zn-MOF was established to have carbon, oxygen, and zinc with ratios of 11.77, 41.73, and 46.50, respectively, as shown in Table 2.

The existence of these compounds proves the success of the development of Mg-MOF-74, Zn-MOF and CuO.

Table 2 Chemical constituents of Mg-MOF-74, CuO and Zn-MOF

Elements	Mass (%)		
	Mg-MOF-74	CuO	Zn-MOF
O	53.631	18.79	41.73
Mg	27.051	-	-
C	18.570	4.50	11.77
K	0.353	-	-
Ca	0.395	1.10	-
Cu	-	43.00	-
Cl	-	27.90	-
Fe	-	4.71	-
Zn		-	46.50

3.1.3 X-ray Diffraction Analysis (XRD)

XRD configurations for the adsorbents-synthesized Mg-MOF-74, Zn-MOF and CuO are demonstrated in Figures 2(a) and (b). As revealed in Figure 2(a), the diffraction pattern of Mg-MOF-74 was matched well with that study as reported in the literature [20]. The development of Mg-MOF-74 was proven by the existence of the characteristic bands at 12.63°, and 18.98° in XRD pattern (blue line). The appearance of these characteristic peaks suggested the successful preparation of Mg-MOF-74. The existence of diffraction bands at 25.5927°, 35.4036°, 37.9819°, and 42.8128° suggest the formation of magnesium oxide, magnesium nitrate hydroxide hydrate and magnesium hydroxide during the preparation of the adsorbent. Furthermore, sharp peaks in this pattern confirm the crystalline structure of Mg-MOF-74.

While as for Zn-MOF, the main bands in the flake-shaped MOF diffraction pattern were found at 2-theta values of nearly 10.94°, 13.58°, 16.49°, 18.92°, 23.04°, 25.27°, 28.75° and 30.17° which efficiently match with simulated XRD configurations, displaying that the pattern come to an agreement with the literature studies [21, 22]. Based upon XRD findings, we were able to detect that Zn-MOF derived from

zinc nitrate is characterized by strong bands, indicating the high crystalline character of the Zn-MOF adsorbent obtained.

Figure 2b displays the XRD spectrum of CuO adsorbent. The XRD patterns exhibit two main peaks at 2θ=32.87° and 2θ=40.23° that can be ascribed to the formation of the CuO crystal phase.

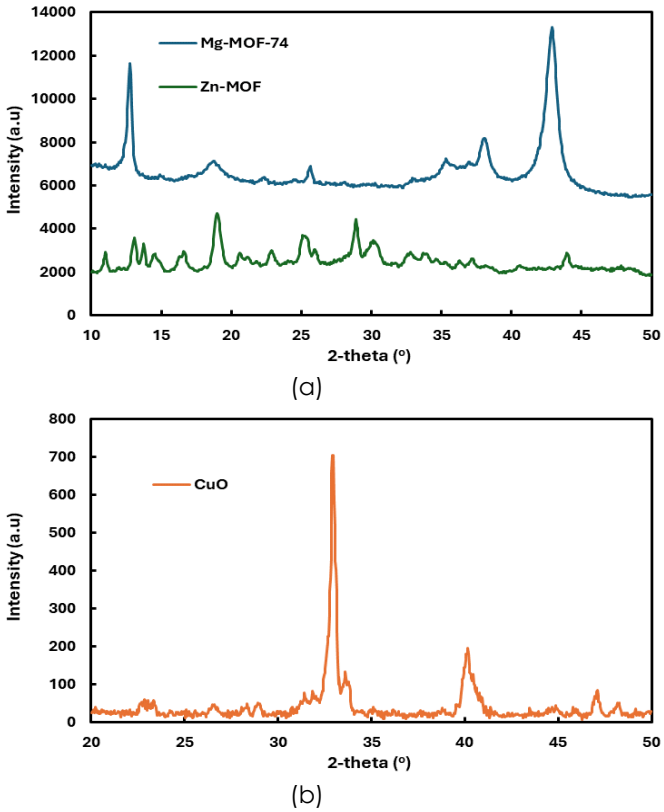

Figure 2 XRD images of (a) Mg-MOF-74 (blue line) and Zn-MOF (grey line) and (b) CuO (orange line)

3.1.4 Thermogravimetric Analysis (TGA)

The TGA profiles for prepared adsorbents are illustrated in Figure 3 with limit of the temperature within 0 to 900 ℃ in N_2 atmosphere at a constant heating rate of 5 ℃/min. As shown in Figure 3, there are two stages of degradation that occurred in Mg-MOF-74 (blue line). The first step in heat degradation is the elimination of the solvent (DMF or trapped water molecules) [23]. The minimum weight loss (8.936%) at first stage indicates that Mg-MOF-74 is stable up to this range of temperature (125.09 ℃). The severe mass decrease began at 310.71℃, which is due to the continuous decomposition of the organic ligand accompanied by the reduction of Magnesium [23]. A total degradation of 40 % of Mg-MOF-74 adsorbent occurred at 500 ℃.

In the TGA curve, mass loss under 200 °C was assigned to the discharge of humidity, water as well as organic solvents physically adsorbed by the samples. In Zn-MOF, approximately 20% of the mass loss occurs in the early stages at temperatures between 0 and 200 °C. The following mass loss (44%) in the span of 200 to 600 °C area might be correlated to the degradation of the ligand of 2,5-dihydroxyterephthalic acid (DHTA). Furthermore, mass loss at 400 °C is indicative of structural decomposition. A fundamental fact regarding the properties of Zn-MOF corresponds to the thermal stability of the material up till 200 °C. As a result, this material can be applied in a variety of adsorption process environment up till 200 °C.

The thermal stability of the porous CuO sample analyzed by TGA can be seen in Figure 3 (orange line). The TGA findings depict that there are two weight losses between 100 and 300 °C. The preliminary mass loss of about 40 % is because of the loss of humidity contents. The following weight loss in the 300-775 °C range is due to the breaking down of the framework of the CuO material.

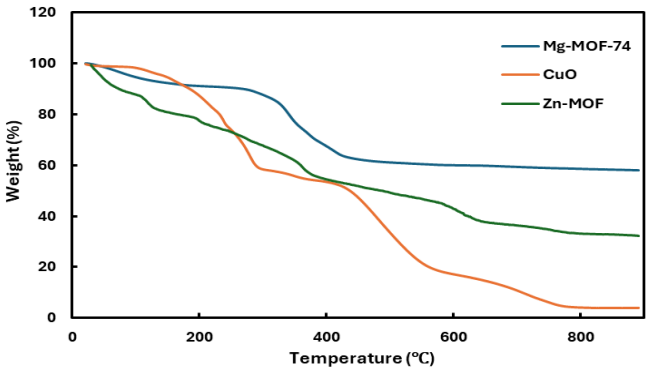

Figure 3 TGA images of Mg-MOF-74, Zn-MOF and CuO

3.1.5 Fourier Transform-Infrared Spectroscopy (FTIR)

The chemical bond and adsorbent functional groups were evaluated by applying FTIR (Model Perkin Elmer FTIR-comm, US) at wavelengths between 4000 and 600 cm^{-1} as presented in Figure 4. The FTIR result of Mg-MOF-74 (blue line) indicates a notable peak at 3420.80 cm^{-1} which is preferable to the hydroxyl group of H-bonded OH broad stretching. Additionally, the absorption peak at 1327.18 cm^{-1} appeared in the Mg-MOF-74 was assigned to the C=O carboxyl groups. The existence of carboxyl functional groups contributes to the 'breathing effect' as a result from the intraframework interaction which enhances the CO_2 uptake capability of the material [24]. The "breathing effect" in metal-organic frameworks (MOFs) refers to the structural flexibility of the framework in response to external stimuli such as gas adsorption, temperature changes, or pressure variations. This phenomenon is particularly relevant in flexible MOFs, where the material undergoes a reversible transformation in its pore structure, expanding or contracting without losing its overall crystallinity. This structural flexibility allows the material to dynamically adjust its pore architecture, making it highly efficient for gas storage and separation applications. The presence of

carboxyl groups enhances the breathing effect by increasing hydrogen bonding and electrostatic interactions between the framework and adsorbed CO_2. When gases such as CO_2 are introduced, their interaction with functional groups in the framework such as carboxyl (-COOH) groups leads to a conformational change in the structure. This can cause pore expansion (open phase) to accommodate more gas molecules or contraction (closed phase) after desorption. These interactions contribute to a more pronounced structural flexibility, allowing the MOF to dynamically adapt and optimize gas uptake. Structural flexibility enables the MOF to preferentially adsorb CO_2 over other gases, making it useful in carbon capture applications [25, 26].

The Zn-MOF configuration obtained was attributed to specific band peaks, which come to an agreement with the previous studies [27]. In Zn-MOF, the bands demonstrate peaks at 3353.91 cm^{-1} might be denoted by the high wave number that the stretching of the metallic cation and water molecule vibrations is associated with the hydroxyl group. Peaks of 804.02 to 2380.23 cm^{-1} could be attributed to symmetric stretching vibrations of the carboxylate cluster, suggesting Zn-MOF crystal formation.

Figure 4 shows the FT-IR band of the synthesized copper oxide sample. The peaks at 2812, 3029.39, 3129.06, 3312.01 and 3341.35 cm^{-1} appointed to the symmetric and asymmetric stretching vibration of the O–H bond. Peaks at 2114.35 and 1994.92 cm^{-1} correspond to C=O stretching of amides and O-H stretching of phenolic compound respectively. Appearance of the peaks at 1592.94, 1397.84 and 1274.770 cm^{-1} indicate stretching vibrations of the Cu–O bond of CuO particles. The existence of bands at 984.61, 894.72 and 824.48 cm^{-1} indicate unique modes of bending vibration of the Cu–O bond [28].

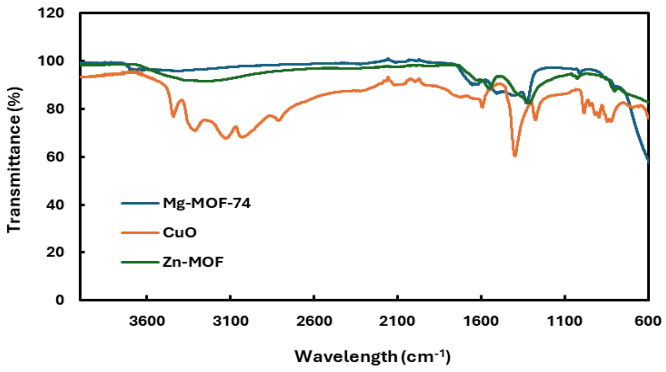

Figure 4 FTIR images of Mg-MOF-74, Zn-MOF and CuO

3.1.6 Brunauer Emmett Teller (BET)

The nitrogen physisorption isotherms of the synthesized samples were measured by nitrogen adsorption–desorption multipoint at 77 K. The results are presented in Figure 5 and Table 3. The isotherms of all materials are of type IV with H3 hysteresis loop corresponding to the IUPAC classification, which indicates the existence of mesoporosity in all prepared samples. The corresponding specific surface area, pore volume and mean pore size of the adsorbents are recorded in Table 3. The specific surface area of Mg-MOF-74 is greater than that of the other samples which would be due to the higher mesopore volume of this material as well as the smaller crystal size. The high surface area is conductive to the CO_2 uptake. The exterior surface area of Mg-MOF-74 calculated was approximately 48.21 % greater than that of Zn-MOF and 85.36 % greater than that of CuO (Table 3). The exterior surface area and mesopore volume of CuO were the lowest. Figure 5 illustrates the isotherm linear plot for CO_2 uptake and desorption of the various synthesized adsorbent samples. According to the IUPAC classification, [29] pores are classified as mesopores with pore diameters of 2 to 50 nm. As can be observed from Table 3, pore sizes around 6.5-15.86 nm occur for all samples.

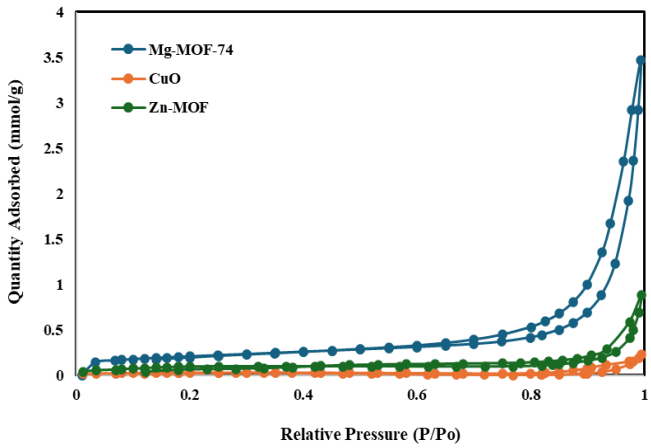

Figure 5 N_2 adsorption-desorption isotherms for Mg-MOF-74, CuO and Zn-MOF

Table 3 The BET exterior surface area, pore size and pore volume of the formulated adsorbents

Adsorbent	BET surface area ($m^2\ g^{-1}$)	Pore size (Å)	Pore volume ($cm^3\ g^{-1}$)
Mg-MOF-74	16.8118	158.5542	0.066639
Zn-MOF	8.7069	65.5707	0.014273
CuO	2.4619	71.2481	0.004385

3.2 CO_2 Adsorption

Runs of tests were executed to study the impact of the amount of adsorbent and operational pressure on the CO_2 uptake process. The work was carried out by varying the adsorbents amount between 0.2-0.6 g at operating pressure 1.0 bar and ambient temperature 27 ℃ respectively. As for the effect of operating pressure, the pressure varied from the range of 1 to 4 bars at room temperature. All the findings obtained are considered in the subsequent segments.

3.2.1 Impact of Adsorbent Dosage

Figure 6 depicts the influence of changing amounts of Mg-MOF-74, Zn-MOF and CuO on CO_2 uptake process.

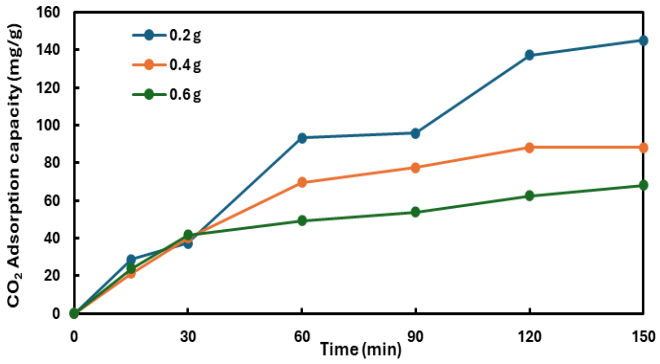

(a)

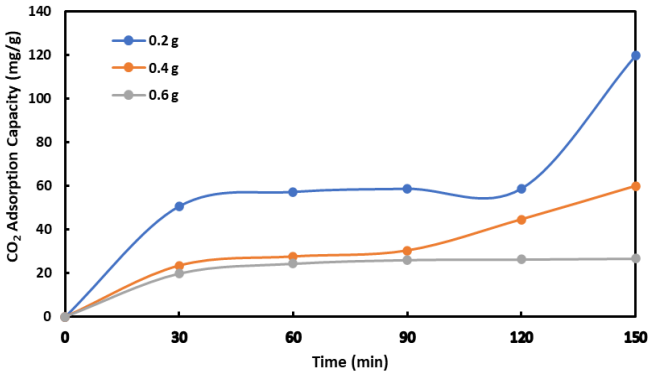

(b)

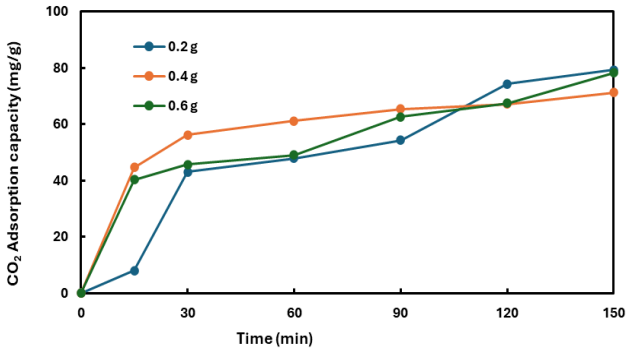

(c)

Figure 6 CO_2 Adsorption capacity for effect of dosage for (a) Mg-MOF-74, (b) Zn-MOF and (c) CuO

The experiment was carried out at a fixed pressure 1.0 bar and ambient temperature. Based on the results obtained in Figure 6, adsorption capacity of the adsorbent decreases as the amount of dosage is increased whereby other parameters are kept constant. The trend is consistent with previous studies. For example, Foo and Hameed [30] reported that excessive adsorbent dosage leads to particle overcrowding, which reduces the availability of active adsorption sites and lowers the adsorption capacity per unit mass. Similarly, Wang *et al*. [31] observed that at higher dosages, agglomeration of adsorbent particles leads to a decrease in the effective surface area, thereby limiting adsorption efficiency.

Our results further substantiate these findings, demonstrating that at a dosage of 0.2 g, Mg-MOF-74 exhibited the highest adsorption capacity (145.09 mg/g), followed by Zn-MOF (119.82 mg/g) and CuO (78 mg/g) within 150 minutes of adsorption time. This trend aligns with the findings of Li *et al*. [32], who reported a similar decrease in adsorption capacity with increasing adsorbent dosage in MOF-based systems, attributing it to the shielding of active sites due to particle clustering [33]. Aggregation of particles will also take place and consequently the available adsorption sites may decrease resulting in lower CO_2 adsorption capacity [34]. Thus, the lowest adsorbent dosage (0.2 g) has the highest adsorption capacity. By highlighting the optimal dosage for maximum adsorption efficiency, our findings contribute to the optimization of adsorbent utilization in gas capture applications, particularly in CO_2 sequestration and environmental remediation. These insights are valuable for scaling up adsorption-based technologies while minimizing material waste and improving process efficiency.

Mg-MOF-74 shows a better adsorption uptake of CO_2 in comparison to all adsorbents prepared in this study. The superior CO_2 adsorption performance of Mg-MOF-74 observed in this study aligns with previous research, which highlights the role of functional groups and surface area in adsorption capacity. Studies have shown that metal-organic frameworks (MOFs) with a high density of open metal sites and functional groups, such as -COOH, significantly enhance CO_2 uptake [35, 36]. The presence of free and available carboxyl (-COOH) groups in Mg-MOF-74 facilitates physical adsorption by providing additional interaction sites for CO_2 molecules, further improving adsorption efficiency [37].

Additionally, the surface area of an adsorbent plays a crucial role in determining adsorption capacity. The larger specific surface area of Mg-MOF-74 (16.1695 m^2/g) compared to Zn-MOF (8.7069 m^2/g) and CuO (2.4619 m^2/g) supports the higher CO_2 uptake observed. Previous studies have similarly reported that higher surface areas and pore volumes enhance gas adsorption efficiency [38]. Our findings agree with the work of Caskey *et al*. [39], who demonstrated that Mg-MOF-74 exhibits exceptional CO_2 uptake due to its high surface area and strong CO_2-framework interactions. The contribution of this study to the field lies in reinforcing the importance of surface characteristics and functional groups in determining CO_2 adsorption efficiency. By directly comparing different adsorbents under controlled conditions, our results offer valuable insights into material selection for CO_2 capture applications. The findings further support the development of MOF-based adsorbents for practical gas separation

processes, particularly in carbon capture technologies, where optimizing adsorption capacity and material efficiency are critical for large-scale implementation.

3.2.2 Impact of Pressure

Impact of pressure upon CO_2 uptake is a vital influence for the real application performance of the adsorbent; thus, the impact of pressure was examined, and findings were shown in Figure 7. The quantity of CO_2 adsorbed was determined for different operating pressure within 150 minutes of adsorption time. The observed increase in CO_2 adsorption capacity with rising operating pressure aligns with findings from previous studies. Several researchers have reported that increasing pressure enhances gas adsorption due to the higher frequency of gas molecules colliding with the adsorbent surface, leading to improved pore filling and adsorption efficiency [37, 40]. For instance, Caskey *et al.* [39] demonstrated that Mg-MOF-74 exhibits a significant increase in CO_2 uptake at higher pressures, attributing it to the strong interaction between CO_2 molecules and open metal sites within the MOF structure. Similarly, Mason *et al.* [38] reported that the adsorption capacity of MOF-based adsorbents follows a pressure-dependent trend, where moderate pressure conditions (e.g., 2–3 bar) optimize adsorption without causing excessive saturation or diffusion limitations.

Our findings further support these observations, as the results indicate that 2 and 3 bar are the optimal operating pressures for CO_2 adsorption across Mg-MOF-74, Zn-MOF, and CuO. This trend can be explained by the increase in gas particle collisions with the adsorbent surface, leading to higher adsorption rates. However, excessive pressure may lead to saturation, where additional pressure does not significantly enhance uptake due to limited available adsorption sites [35].

In addition, the CO_2 uptake capability of the materials is mostly subject to aspects, for instance specific surface area, pore size, and pore volume. Adsorption capacity increases in the direction CuO < Zn-MOF< Mg-MOF-74, reaching, accordingly, 78.59 mg/g, 125 mg/g, 149.70 mg/g. Mg-MOF-74 shows better adsorption uptake of CO_2 in comparison to all MOFs prepared in this study. The form of the isotherm exposes that the prepared Mg-MOF-74 is mesoporous structure with highest surface area (16.1965 m^2/g) (refer Table 3). As exterior areas rise with rising pressure, a lot of active sites are accessible, heading to greater uptake of CO_2. Moreover, the effect of the exterior area is essential in CO_2 uptake process [30]. This shows that other factors have an impact on CO_2 adsorption.

Understanding the relationship between pressure and adsorption performance is critical for designing efficient CO_2 capture systems, particularly for industrial applications where pressure conditions can be optimized to maximize adsorption efficiency while minimizing energy costs. Furthermore, the comparative analysis of Mg-MOF-74, Zn-MOF, and CuO under varying pressure conditions offers valuable insights into the performance of different materials, aiding in the selection of the most suitable adsorbent for specific applications.

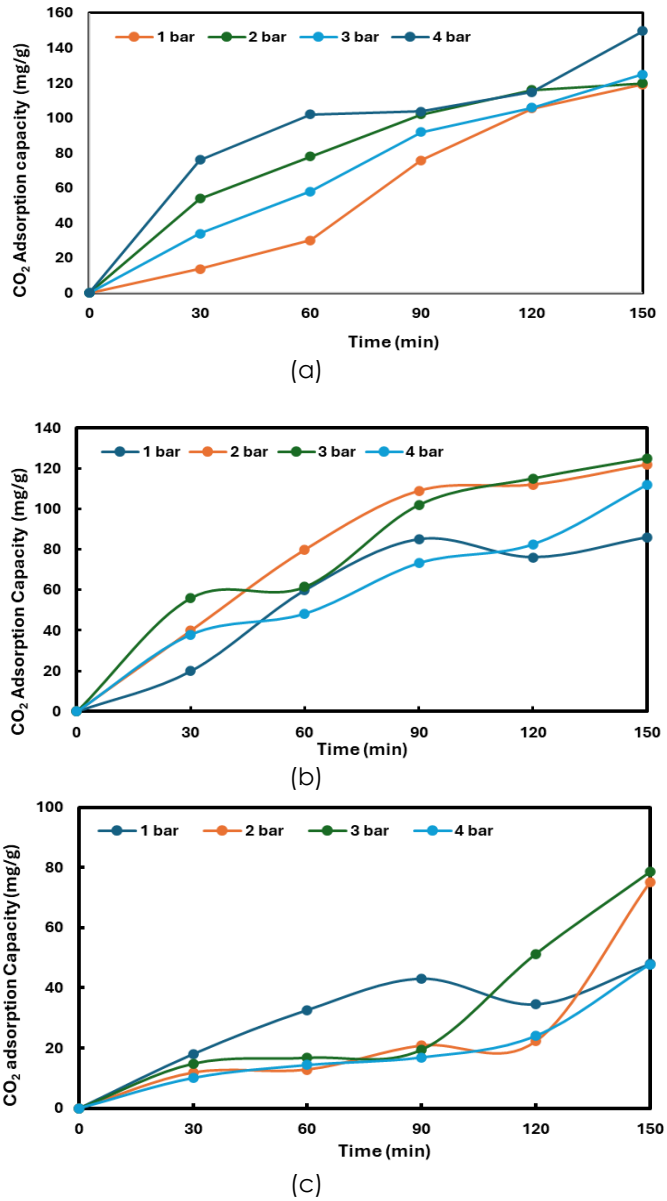

Figure 7 CO_2 adsorption uptake for the influence of pressure for (a) Mg-MOF-74, (b) Zn-MOF and (c) CuO

4.0 CONCLUSIONS

In this study, Mg-MOF-74, Zn-MOF, and CuO adsorbents were synthesized and evaluated for their effectiveness in carbon capture and sequestration. The structural integrity of the synthesized materials was confirmed, with Mg-MOF-74 and Zn-MOF retaining their characteristic crystalline forms, ensuring their suitability for adsorption applications. The significant findings of this study highlight that

MOF-based adsorbents, particularly Mg-MOF-74, exhibit superior CO_2 adsorption performance compared to metal oxides. Mg-MOF-74 demonstrated the highest CO_2 uptake due to its larger specific surface area (16.1695 m^2/g) and the presence of free -COOH groups, which enhance physical adsorption interactions. In contrast, Zn-MOF and CuO displayed lower adsorption capacities, suggesting that MOF-based adsorbents hold greater promise for efficient CO_2 capture. Key operational parameters, including pressure and adsorbent dosage, were found to substantially influence adsorption performance. The study determined that an optimal operating pressure of 2–3 bar maximized CO_2 uptake across all adsorbents, as increasing pressure enhanced gas collisions with the adsorbent surface and improved pore filling. However, excessive pressure beyond this range may lead to saturation effects, limiting additional adsorption. Furthermore, adsorbent dosage played a crucial role, with 0.2 g identified as the optimal amount for maximizing adsorption capacity. Increasing the dosage beyond this threshold led to a decline in adsorption efficiency due to the overlapping of adsorption sites and particle overcrowding.

While this study provides valuable insights into the performance of Mg-MOF-74, Zn-MOF, and CuO for CO_2 capture, further research is necessary to explore key aspects such as temperature effects, long-term stability, hybrid adsorbents, real-world applications, and kinetic and isotherm modeling. This research contributes to the ongoing development of efficient adsorbents for CO_2 capture, laying the foundation for future advancements in sustainable carbon sequestration technologies.

Acknowledgements

This study is completely funded by FRGS grant, No. FRGS/1/2021/TK0/UMP/02/79 (University reference RDU210150). The authors fully acknowledged Ministry of Higher Education (MOHE) and Universiti Malaysia Pahang Al-Sultan Abdullah for the granted fund which leads this valuable study feasible and valuable.

Conflicts of Interest

The authors declare that there is no conflict of interest regarding the publication of this paper.

References

[1] Dan, T., Qiang, Z., Yixuan, Z., Ken, C., Christine, S., Chaopeng, H., Yue, Q. and Steven, J. D. 2019. Committed Emissions from Existing Energy Infrastructure Jeopardize 1.5 °C Climate Target. *Nature*. 572: 373–377. Doi: https://doi.org/10.1038/s41586-019-1364-3.

[2] Anderson, T. R., Hawkins, E. and Jones, P. D. 2016. CO_2 the Greenhouse Effect and Global Warming: From the Pioneering Work of Arrhenius and Callendar to Today's Earth System Models. *Endeavour*. 40(3): 178–187. Doi: https://doi.org/10.1016/j.endeavour.2016.07.002.

[3] Songolzadeh, M., Ravanchi, M. T. and Soleimani, M. 2012. Carbon Dioxide Capture and Storage: A General Review on Adsorbents. *World Academy of Science, Engineering and Technology International Journal of Chemical and Molecular Engineering*. 6(10): 900–907.

[4] Christophe, J., Yuen, L., Anderson, C. J., Xiao, G., Webley, P. A. and Hoadley, A. F. A. 2016. Multi-objective Optimisation of Hybrid Vacuum Swing Adsorption and Low-Temperature Post-Combustion CO_2 Capture. *Journal of Cleaner Production*. 11: 193–203. Doi: 10.1016/j.jclepro.2015.08.033.

[5] Bui, M. 2018. Carbon Capture and Storage (CCS): The Way Forward. *Energy & Environmental Science*. 11(5): 1062–1176.

[6] Pu, H. H., Rhim, S. H., Gajdardziksa-Josifovska, M., Hirschmugl, C. J., Weinert, M. and Chen, J. H. 2014. A Statistical Thermodynamics Model for Monolayer Gas Adsorption on Graphene-Based Materials: Implications for Gas Sensing Applications. *RSC Advances*. 4(88): 47481–47487.

[7] Ali, R. S., Meng, H., Li, Z. 2022. Zinc-Based Metal-Organic Frameworks in Drug Delivery, Cell Imaging, and Sensing. *Molecules*. 27(1): 1–27. Doi: https://doi.org/10.3390/molecules27010100.

[8] Bosoaga, A., Masek, O. and Oakey, J. E. 2009. CO_2 Capture Technologies for Cement Industry. *Energy Procedia*. 1(1): 133–140. Doi: 10.1016/j.egypro.2009.01.020.

[9] Son, S. R., Go, K. S. and Kim, S. D. 2009. Thermogravimetric Analysis of Copper Oxidefor Chemical-Looping Hydrogen Generation. *Industrial & Engineering Chemistry Research*. 48(1): 380–387. Doi: 10.1021/ie800174c.

[10] Da-Ae, Y., Hye-Young, C., Kim, J., Seung-Tae, Y. and Wha-Seung, A. 2012. CO_2 Capture and Conversion using Mg-MOF-74 Prepared by a Sonochemical Method. *Energy & Environmental Science*. 5: 6465–6473.

[11] Bao, Z., Yu, L., Ren, Q., Lu, X., Deng, S. 2011. Adsorption of CO_2 and CH_4 on a Magnesium-based Metal Organic Framework. *Journal of Colloid and Interface Science*. 353(2): 549–556.

[12] Cheng, L. W. and Ridzuan, D. 2014. Synthesis, Characterization and Modification of Metal Organic Framework-74 for CO_2 Adsorption. Thesis. Universiti Teknologi PETRONAS.

[13] Tapiador, J., Leo, P., Rodríguez Diéguez, A., Choquesillo, D. L., Calleja, G. and Gisela, O. 2022. A novel Zn-based-MOF for Efficient CO2 Adsorption and Conversion under Mild Conditions. *Catalysis Today*. 390–391(1): 230–236.

[14] Zou, L., Yuan, J., Yuan, Y. Gu, J., Li, G., Zhang, L. and Liu, Y. 2019. A Zn(II) Metal–organic Framework Constructed by a Mixed-ligand Strategy for CO_2 Capture and Gas Separation. *CrystEngComm*. 21: 3289–3294.

[15] Wang, C., Wang, Z., Yu, J., Lu K., Bao, W., Wang, G., Peng, B., Peng, W. and Yu, F. 2023. Facile Synthesis Behavior and CO_2 Adsorption Capacities of Zn-based Metal Organic Framework Prepared via a Microchannel Reactor. *Chemical Engineering Journal*. 454(1): 140078.

[16] Ávila-López, M. A., Luévano-Hipólito and E., Torres-Martínez, L. M. 2019. CO_2 Adsorption and Its Visible-light-driven Reduction using CuO Synthesized by an Eco-friendly Sonochemical Method. *Journal of Photochemistry and Photobiology A: Chemistry*. 382: 111933.

[17] Isahak, W. N. R. W., Ramli, Z. A. C., Ismail, M. W., Ismail K., Yusop, R. M., Hisham, M. W. M. and Yarmo, M. A. 2013. Adsorption–desorption of CO_2 on Different Type of Copper Oxides Surfaces: Physical and Chemical Attractions Studies. *Journal of CO_2 Utilization*. 2: 8–15.

[18] Xin, C., Ren, Y., Zhang, Z., Liu, L., Wang, X., and Yang, J. 2021. Enhancement of Hydrothermal Stability and CO2Adsorption of Mg-MOF-74/MCF Composites. *ACS Omega*. 6(11): 7739–7745. https://doi.org/10.1021/ACSOMEGA.1C00098.

[19] Campbell, J. and Tokay, B. 2017. Controlling the Size and Shape of Mg-MOF-74 Crystals to Optimise Film Synthesis on Alumina Substrates. *Microporous and Mesoporous Materials*. 251: 190–199.

[20] Li, L. 2021. Synthesis and Catalytic Properties of Metal-organic Frameworks Mimicking Carbonic Anhydrase. *Digitalcommons*. 924: 1–21.

[21] Bagheri, N., Khataee, A., Habibi, B. and Hassanzadeh, J. 2018. Mimetic Ag Nanoparticle/Zn-based MOF Nanocomposite (AgNPs@ZnMOF) Capped with Molecularly Imprinted Polymer for the Selective Detection of Patulin. *Talanta*. 179: 710–718. Doi: 10.1016/j.talanta.2017.12.009.

[22] Yang, D. A., Cho, H. Y., Kim, J., Yang, S. T., and Ahn, W. S. 2012. CO_2 capture and conversion using Mg-MOF-74 prepared by a sonochemical method. *Energy & Environmental Science*. 5(4): 6465–6473. https://doi.org/10.1039/C1EE02234B.

[23] Serre, C., Bourrelly, S., Vimont, A., Ramsahye, N. A., Maurin, G., Llewellyn, P. L., Daturi, M., Filinchuk, Y., Leynaud, O., Barnes, P., and Férey, G. 2007. An Explanation for the Very Large Breathing Effect of a Metal-organic Framework during CO_2 adsorption.

[24] Férey, G., Serre, C., Mellot-Draznieks, C., Millange, F., Surblé, S., & Dutour, J. 2004. A Hybrid Solid with Giant Pores Prepared by a Combination of Targeted Chemistry, Simulation, and Powder Diffraction. *Angewandte Chemie International Edition*. 43(46): 6296–6301

[25] Coudert, F. X. 2015. Responsive Metal–organic frameworks and Framework Materials: Under Pressure, Taking the Heat, in the Spotlight, with Friends. *Chemical Materials*. 27(6): 1905–1916

[26] Sacourbaravi, R., Ansari-As, Z., Kooti, M., Nobakht, V. and Darabpour, E. 2020. Fabrication of Ag NPs/Zn-MOF Nanocomposites and Their Application as Antibacterial Agents. *Journal of Inorganic and Organometallic Polymers and Materials*. 30(11): 1–7. Doi:10.1007/s10904-020-01601-x.

[27] Raul, P. K., Senapati, S., Sahoo, A. K., Umlong, I. M., Devi, R. R., Thakur, A. J. and Veer V. 2014. CuO Nanorods: a Potential and Efficient Adsorbent in Water Purification. *RSC Advances*. 4: 40580.

[28] Kahr, J., Morris, R. E. and Wright, P. 2013. A Post Synthetic Incorporation of Nickel into CPO-27(Mg) to Give Materials with Enhanced Permanent Porosity. *Cryst Eng Comm*. 15: 9779. Doi: 10.1039/c3ce41228h.

[29] Foo, K. Y., and Hameed, B. H. 2012. Insights into the modeling of Adsorption Isotherm Systems. *Chemical Engineering Journal*. 156(1): 2–10.

[30] Wang, J., Chen, Z., Chen, B., and Zhao, Y. 2019. Adsorption Behaviors of Metal-organic Frameworks for Gas Separation and Purification. *Environmental Science & Technology*. 53(4): 2175–2183.

[31] Li, X., Ma, J., Zhang, L., and Liu, H. 2020. Influence of Adsorbent Dosage on Adsorption Performance: A Case Study of MOFs for CO_2 Capture. *Journal of Colloid and Interface Science*. 565: 210–220.

[32] Adhikari, A. K. and Lin, K. S. 2014. Synthesis, fine Structural Characterization, and CO_2 Adsorption Capacity of Metal Organic Frameworks-74. *Journal of Nanoscience and Nanotechnology*. 14(4): 2709–2717. Doi: 10.1166/jnn.2014.8621.

[33] Dien, N. D. 2019. Preparation of Various Morphologies of ZnO Nanostructure through Wet Chemical Methods. *Advanced Material Science*. 4: 147. Doi: https://doi.10.15761/AMS.1000147.

[35] Zhou, H. C., Kitagawa, S., & others. 2018. Metal-organic Frameworks (MOFs). *Chemical Society Reviews*. 47(16): 5336–5354.

[36] Yang, D., Liu, B., Zhao, D., & Sun, L. 2020. Functionalized MOFs for CO_2 Capture and Separation. *Chemical Engineering Journal*. 388: 124243.

[37] Li, J. R., Sculley, J., & Zhou, H. C. 2019. Metal-organic Frameworks for Separations. *Chemical Reviews*. 112(2): 869–932.

[38] Mason, J. A., Sumida, K., Herm, Z. R., Krishna, R., & Long, J. R. 2015. Evaluating Metal-organic Frameworks for Post-combustion Carbon Dioxide Capture Via Temperature Swing Adsorption. *Energy & Environmental Science*. 4(8): 3030–3040

[39] Caskey, S. R., Wong-Foy, A. G., & Matzger, A. J. 2008. Dramatic Tuning of CO_2 Uptake via Metal Substitution in a Coordination Polymer with Cylindrical Pores. *Journal of the American Chemical Society*. 130(33): 10870–10871.

[40] Wang, J., Chen, Z., Chen, B., & Zhao, Y. 2020. Adsorption Behaviors of Metal-Organic Frameworks for Gas Separation and Purification. *Environmental Science & Technology*. 53(4): 2175–2183.

.